

ANALYSIS OF THE POGO VIBRATION

by

William T. Thomson

Professor of Mechanical Engineering
University of California, Santa Barbara

Introduction

Engineering systems are often assembled from a number of independent components which must function harmoniously according to the desired performance of the overall system. Although each component may function satisfactorily by itself, an assembly of such components may fail to meet the desired overall requirements. It is therefore necessary to examine such an assembly of components from the point of view of the system objectives.

System engineering is an approach which recognizes the many variables of the system and interrelates them to the overall function of the system. The objectives of the system may be diverse aims such as low cost, reliability, vibration-free operation, or any other requirement to be specified. To attain the system objectives, modification of the subfunctions of the components may be required. If the system is to be optimized for a given performance, the effect of variation of each of the variables in the system must be examined. Of frequent concern is the question of system stability. Thus, fundamental aspects of many fields may be involved in a systems study.

(c) 1967 by the Board of Trustees of the Leland Stanford Junior University.
Prepared with the support of the National Science Foundation.

This report was made possible through the cooperation of the Engineering Mechanics Department of TRW Systems. The author wishes to especially thank Mr. John H. Walker for his valuable comments on the Pogo problem.

The Pogo Problem

One of the interesting examples of systems instability was that encountered by the behavior of the Titan-2 missile shortly after lift-off. The Titan-2 missile is a liquid propellant rocket 103 ft. tall and weighing 165 tons with a first stage thrust of 430,000 lbs. It was designed as a military weapon to carry a nuclear warhead 6,000 miles or more.

When the Gemini program was conceived, the Manned Spacecraft Center decided to use the Titan-2 missile to boost the two-man teams of astronauts into orbit. However, serious vibration problems had to be overcome for the booster. After about 100 seconds of flight, severe longitudinal oscillations, called the "Pogo bounce" between 11 and 14 c.p.s., with accelerations up to 5 g's, would develop in the Titan-2. For an unmanned flight such vibrations could be tolerated. However, to an astronaut, such vibration levels spelled trouble. For example, it is known that vibration levels of only 1/2 g at frequencies near 10 c.p.s. would seriously impair one's vision, so that an astronaut subjected to such environment could not read the instrument panel. Moreover, such a ride would be a most unpleasant physiological experience.

This longitudinal oscillation was known to exist in all liquid propellant missiles but its cause and cure were unknown in 1962. Various fixes were proposed and tried, and in one test a 15 million dollar missile was destroyed in flight due to excessive vibrations. After an intensive study program costing 3 million dollars, the troublesome "Pogo bounce" was identified as coupled oscillation between the structure and the rocket-propellant-combustion system. Components when tested separately would behave according to expectation and the difficulties experienced in operation as a system became predictable only by the systems approach of analysis. As in most cases, understanding the cause leads to a cure, and the "Pogo bounce" in the Titan-2 booster was successfully reduced to levels acceptable to the Gemini program.

Systems Analysis of the Liquid Propellant Missile

Figure 1 illustrates the essential components of the Titan-2 propulsion system with only one of the two engines shown. The mono-propellant system shown in Figure 2 is a simplification which will adequately describe the instability known as the Pogo-bounce and illustrates the systems approach to be used. The components of the system are:

- (a) Propellant tank with its liquid propellant
(We will refer to the propellant as fuel, although it could stand for the oxidizer as well.)
- (b) Fuel feed line
- (c) Turbo-pump
- (d) Discharge line and injector
- (e) Rocket engine
- (f) Missile structure

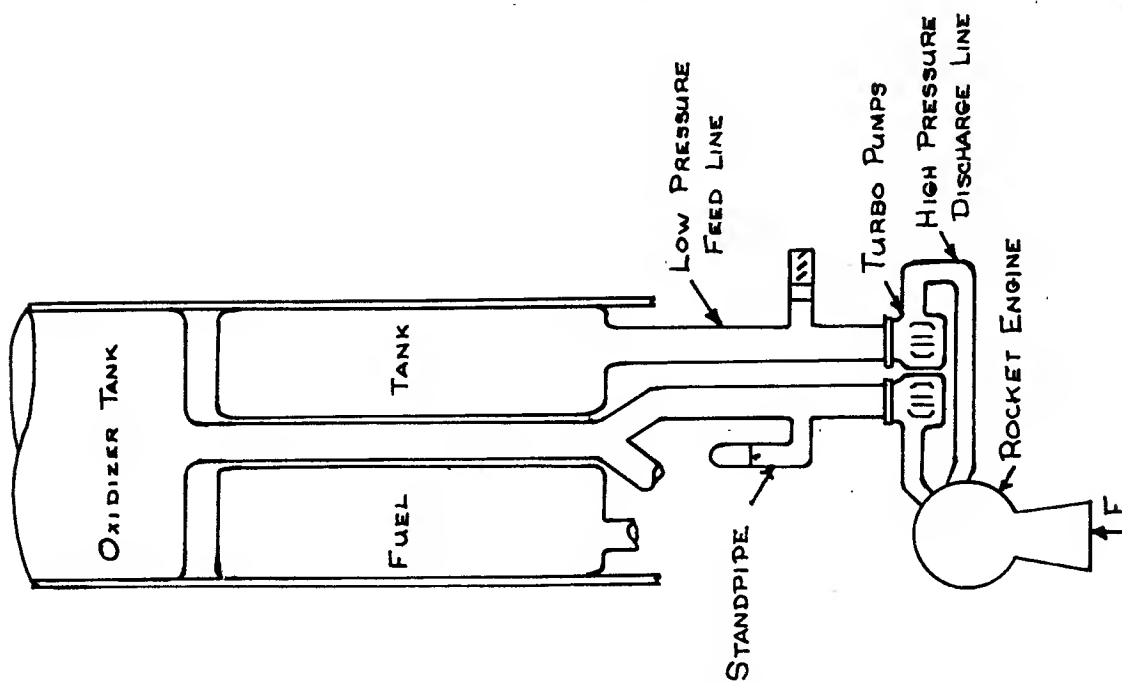


FIG. 1 - TITAN 2 SYSTEM

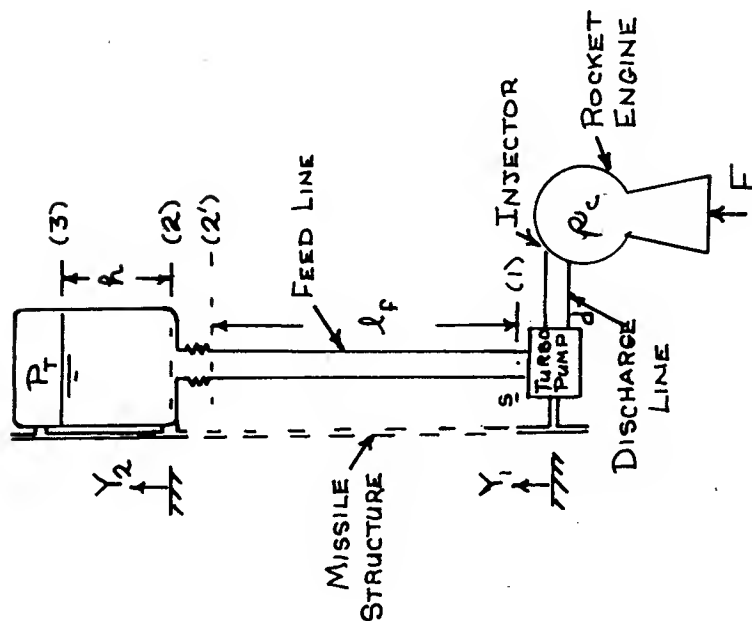
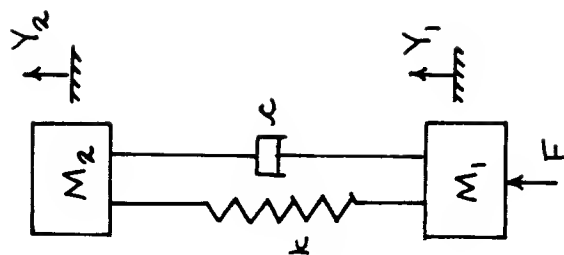


FIG. 2 - SIMPLIFIED SYSTEM



ECL 1005

To simplify the analysis we will lump the mass of the system at two points where the displacements Y_1 and Y_2 are measured from an inertial reference, (assumed to be the Earth). Thus, M_1 will include the mass of the turbo-pump and the rocket engine, while M_2 will represent the variable mass of the fuel in the tank. The two masses are connected by a spring and damper representative of the intervening structure, and the system is to be adjusted to result in the same natural frequencies as the first and second modes of the missile.

The behavior of the system can be briefly described in a qualitative manner as follows. A disturbance in the fuel feed system is transmitted to the injector of the rocket in the form of a pressure variation and a corresponding variation in the fuel flow rate to the combustion chamber. The resulting fluctuation in the thrust introduces a variation in the structural excitation which causes relative motion of the fuel tank with respect to the feed line, the turbo-pump and the engine. With proper phase and period of vibration, the sequence of events described may continue to increase in amplitude to proportions unacceptable to the design.

Pertinent to the problem is the stability of the system performance and how it may be altered by design modifications. The systems approach to be used here is that of establishing the transfer function of each component and assembling these into a block diagram circuit representative of the overall system. Such a circuit may then be analyzed by the various techniques available in the treatment of closed-loop systems.

Component Transfer Function

It is evident that there are several variables to be considered in the system. They can be identified by isolating each component and examining its input and output relationship which will be expressed in terms of a transfer function. For its development we will consider the fluctuation in the quantity under consideration to be a small perturbation from its steady state value and linearize the analysis by ignoring second order terms of the perturbations. The transfer function is then defined by the Laplace transform of the ratio of the output to input with zero initial condition.

(a) Fuel Feed System

The flow rate in the fuel feed system is affected by the acceleration of the structure and the pressure variation in the fuel. Referring to Fig. 2, the tank and its fuel are assumed to have acceleration \ddot{Y}_2 whereas the fuel feed line is assumed to have acceleration \ddot{Y}_1 equal to that of the pump and engine. Sections of this system from the tank to the suction inlet of the pump will be first analyzed by using Newton's second law, Bernoulli's equation, and the continuity principle of mass flow rate. Capital letters will be used to represent the total quantity, which will be separated into its steady state value with an overhead bar and its fluctuation indicated by the lower case letter (i.e. $P = \bar{P} + p$).

Between points (3) and (2) Newtons equation of motion is

$$P_2 - P_T - \gamma h = \frac{\gamma h}{g} \ddot{Y}_2$$

where

$$\begin{aligned} P &= \text{pressure} \sim \text{lbs/ft}^2 \\ \gamma &= \text{weight density of fuel} \sim \text{lbs/ft}^3 \\ h &= \text{head} \sim \text{ft} \\ g &= \text{acceleration of gravity} \sim 32.2 \text{ ft/sec}^2 \\ \ddot{Y}_2 &= \text{absolute acceleration of tank and fuel} \sim \text{ft/sec}^2 \end{aligned}$$

For the steady state condition the missile is accelerating with acceleration \ddot{Y} under steady pressures \bar{P} and we simply obtain the equation

$$\bar{P}_2 - \bar{P}_T - \gamma h = \frac{\gamma h}{g} \ddot{Y}$$

Substituting $P = \bar{P} + p$ and $\ddot{Y} = \ddot{Y} + \ddot{y}$ into the first equation and subtracting out the steady state equation, we arrive at the result

$$p_2 - p_T = \frac{\gamma h}{g} \ddot{y}_2 \quad (1)$$

Next we consider the short section between (2) and (2'). Neglecting the velocity of the fuel in the tank, we assume that Bernoulli's equation can be applied to the nonsteady as well as steady state flow when the perturbations are small.

$$P_2 = \bar{P}_2' + \frac{\gamma}{2g} U_{2'}^2$$

$$\bar{P}_2 = \bar{P}_2' + \frac{\gamma}{2g} U_{2'}^2$$

Here

$$U_{2'} = \bar{U}_{2'} + u_{2'} = \text{flow velocity} \sim \text{ft/sec.}$$

Subtracting and neglecting the second order of the perturbation $u_{2'}^2$, we obtain

$$P_2 = P_{2'} + \frac{\gamma}{g} \bar{U}_{2'} u_{2'}$$

To express this equation in terms of the weight flow rate \dot{W} lb/sec we substitute

$$\gamma A_f U_{2'} = \dot{W}_{2'} = \dot{W}_1 = \bar{\dot{W}}_1 + \dot{w}_1$$

and arrive at the result

$$P_2 = P_{2'} + \left(\frac{\bar{\dot{W}}_1}{\gamma g A_f^2} \right) \dot{w}_1 \quad (2)$$

Continuing from (2') to (1) and assuming a pressure loss due to friction in the form $C_f \frac{\gamma}{2g} U_1^2$, Newton's second law yields

$$P_1 - P_{2'} - \gamma l_f + C_f \frac{\gamma}{2g} U_1^2 = \frac{\gamma l_f}{g} (\ddot{Y}_1 - \dot{U}_1)$$

where the acceleration of the fluid in the line is $(\ddot{Y}_1 - \dot{U}_1)$. Bernoulli's equation for the steady state then becomes

$$\bar{P}_1 - \bar{P}_{2'} - \gamma l_f + C_f \frac{\gamma}{2g} \bar{U}_1^2 = \frac{\gamma l_f}{g} \ddot{Y}_1$$

Recognizing that $\bar{U}_1 = 0$, and $\dot{U}_1 = \dot{u}_1$, the subtraction of the steady state equation yields

$$p_1 - p_{2'} + C_f \frac{\gamma}{g} \bar{U}_1 u_1 = \frac{\gamma l_f}{g} (\ddot{y}_1 - \dot{u}_1)$$

or in terms of the weight flow rate

$$p_1 - p_{2'} + C_f \frac{\bar{W}_1}{\gamma g A_f^2} \dot{w}_1 = \frac{\gamma l_f}{g} (\ddot{y}_1 - \frac{\dot{w}_1}{\gamma A_f}) \quad (3)$$

The quantities p_2 and $p_{2'}$ can now be eliminated from Equations (1) (2) and (3), and letting $p_1 = p_s$ = suction pressure at the pump inlet, the resulting equation is

$$\frac{l_f}{g A_f} \ddot{w}_1 + (C_f + 1) \left(\frac{\bar{W}_1}{\gamma g A_f^2} \right) \dot{w}_1 = p_T - p_s + \frac{\gamma l_f}{g} \ddot{y}_1 + \frac{\gamma h}{g} \ddot{y}_2 \quad (4)$$

Its Laplace transform with zero initial conditions is

$$\left[\frac{l_f}{g A_f} s + (C_f + 1) \left(\frac{\bar{W}_1}{\gamma g A_f^2} \right) \right] \dot{w}_1(s) = p_T(s) - p_s(s) + \frac{\gamma l_f}{g} s^2 y_1(s) + \frac{\gamma h}{g} s^2 y_2(s) \quad (5)$$

It is worthy of mention at this point to call attention to the fact that the left side of Equation (5) is in terms of the inertiance and resistance defined as

$$L = \frac{l}{g A} = \text{inertiance}$$

$$R = C \frac{\bar{W}}{\gamma g A^2} = \text{resistance}$$

The compliance in the above equation is zero since the fluid was assumed to be incompressible.

In order to identify the transfer function for the block diagram, we rearrange Eq. (5) as follows

$$\dot{w}_1(s) = \frac{p_T(s)}{L(s+\alpha)} - \frac{p_S(s)}{L(s+\alpha)} + \frac{\gamma l_f}{g L} \frac{s^2 u_1(s)}{(s+\alpha)} + \frac{\gamma h}{g L} \frac{s^2 u_2(s)}{(s+\alpha)} \quad (6)$$

$$\alpha = \frac{C_f + 1}{L} \left(\frac{\bar{W}_1}{\gamma g A^2} \right)$$

which is represented by the block diagram of Figure 3.

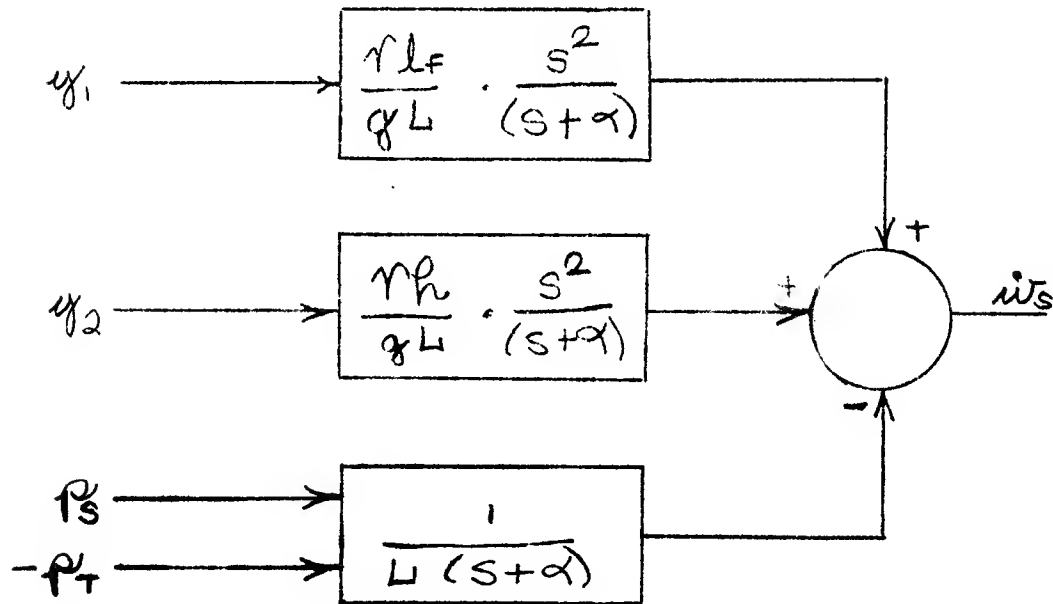


Figure 3- Block Diagram of Fuel Feed System

(b) Turbo Pump Including Cavitation Bubble

The pump performance is limited by cavitation, or the formation of gaseous bubbles which occurs when the fluid pressure at any point becomes less than the vapor pressure of the fluid. Cavitation is most likely to occur at the pump inlet or the leading edge of impeller vanes. Bubbles collapse when the fluid pressure again reaches a value above the vapor pressure. Excessive cavitation will produce fluctuation in the flow rate and erratic combustion in the rocket engine which it supplies.

Fuel entering the pump is accelerated towards the impeller periphery and enters the volute at high speed. The expansion in the volute then converts the large kinetic energy due to velocity into potential energy or pressure head.

Pump characteristics are generally displayed in terms of pressure head rise against the total pressure head at the suction side and the flow rate. Typical curves are shown in Figure 4 and Figure 5. The total pressure head at the suction side is equal to $(P_s + \frac{\gamma}{2g} U^2 - P_{\text{VAPOR}})^{1/\gamma}$ and is called the net positive suction head NPSH.

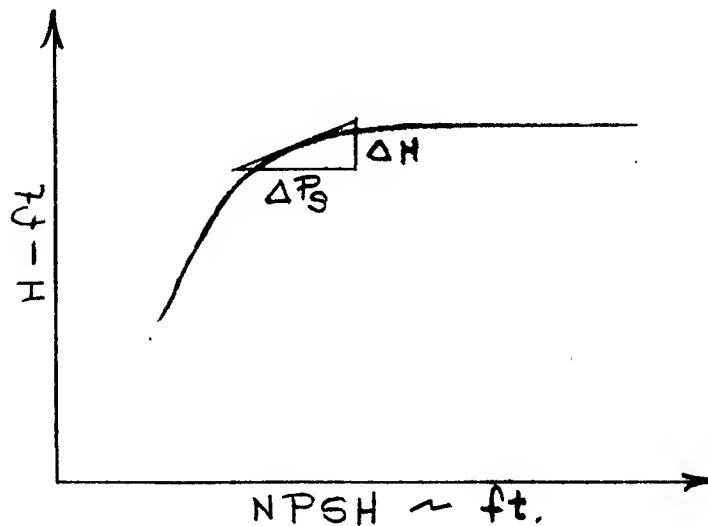


Figure 4 - Head versus Inlet Pressure

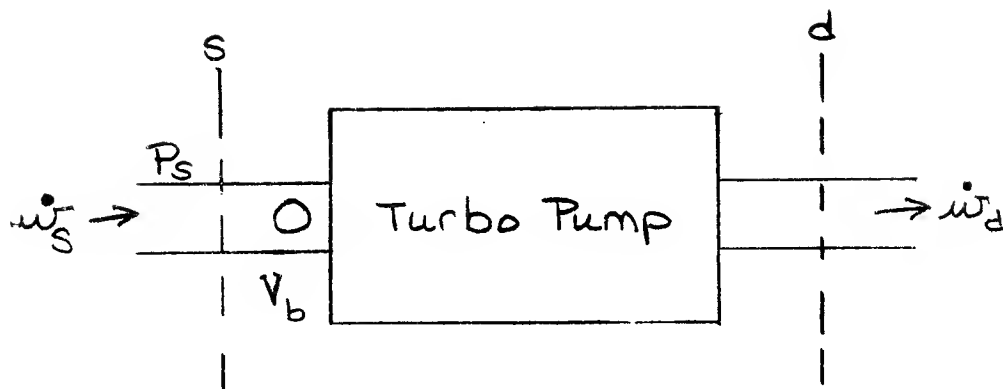


Figure 6 - Pump Flow Rate with Cavitation Bubble

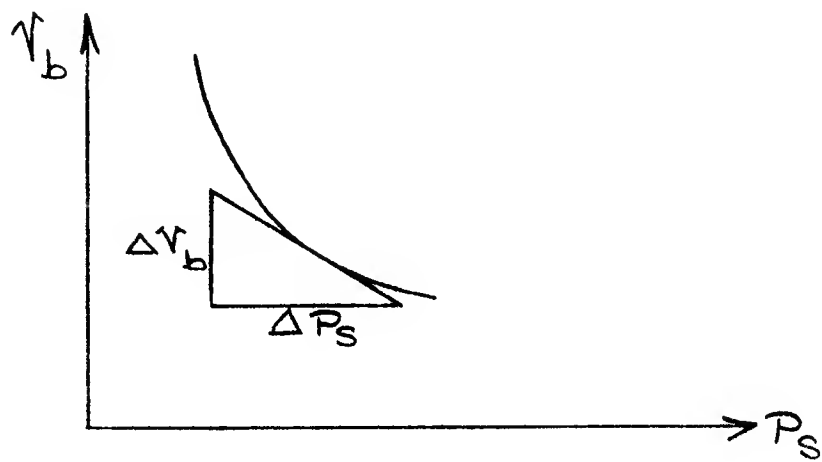


Figure 7 - Volume-Pressure Relation for Cavitation Bubble

Cavitation, or the formation of bubbles at the pump inlet, increases as the NPSH decreases. Assuming the total volume of the bubbles to be V_b we can apply the principle of continuity of weight flow rate between the suction and discharge ends of the pump shown in Figure 6.

$$\dot{w}_d = \dot{w}_s + \rho \dot{V}_b \quad (8)$$

Since the volume V_b is that of a large number of small bubbles which form and collapse in the inlet region, it is doubtful whether a polytropic gas law, such as $P V^n = \text{constant}$, can be applied. However, the relationship between the volume V_b and the suction pressure P_s must be of the general form shown in Figure 7.

The cluster of bubbles in the region of the pump inlet can be viewed as a liquid-gas mixture of large compliance in comparison to that of any liquid itself. Thus, we have a column of liquid supported by this spongy mixture which behaves like a spring and it would be of interest to determine its spring rate K_b .

The spring rate of a mechanical spring is determined by applying an increment in the load and measuring the deformation. Thus, if we assume the cross sectional area of this spongy mixture to be constant and equal to that of the pipe at that point, the spring rate can be expressed as

$$K_b = \frac{-A \Delta P_s}{\Delta x} = \frac{-A^2 \Delta P_s}{\Delta V_b} \quad (9)$$

If P_s is known, then the slope $\frac{\Delta P_s}{\Delta V_b}$ may be found from Figure 7.

The spring rate K_b may also be related to the natural frequency of the liquid column described above. The mass of the supported column is $\frac{\gamma}{g}(l_f + h)$ and hence

$$\omega = \sqrt{\frac{K_b}{\frac{\gamma}{g}(l_f + h)}}$$

A value of K_b corresponding to the first natural frequency of the missile would certainly represent an unfavorable compliance to the system.

To complete the transfer function for the pump including the effect of the cavitation bubbles we obtain from Eq. (9)

$$\dot{V}_b = \frac{-A^2 \dot{p}_s}{K_b}$$

Eq. (8) can then be written as

$$\dot{w}_d = \dot{w}_s - \frac{\gamma A_f^2}{K_b} \dot{p}_s \quad (10)$$

Taking the Laplace transform of Eqs. (7) and (10) the transfer functions for the pump and the cavitation become

$$p_d(s) = (a+1) p_s(s) - R_p \dot{w}_d(s) \quad (11)$$

$$\dot{w}_d(s) = \dot{w}_s(s) - \frac{\gamma A_f^2}{K_b} s p_s(s) \quad (12)$$

The block diagram representing these equations is shown in Figure 8.

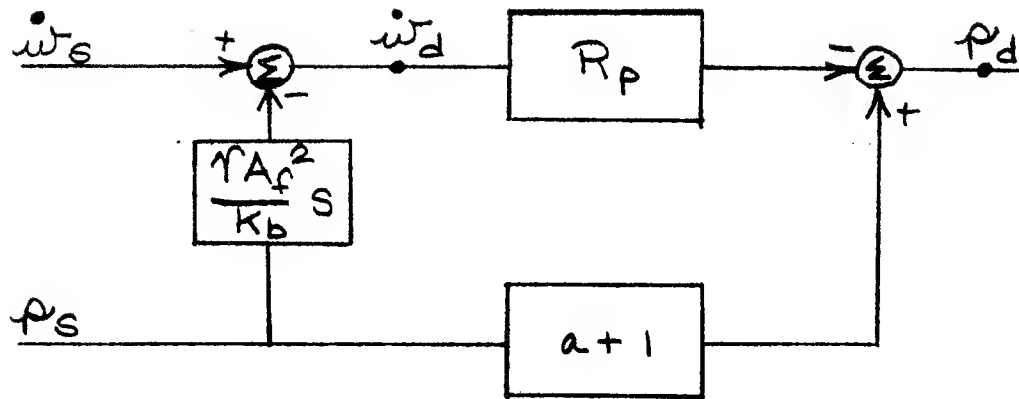


Figure 8 - Block Diagram of Turbo-Pump Including Cavitation Bubble

(c) Discharge Line and Injector

The discharge line carries the fluid under high pressure from the turbo-pump to the injector and combustion chamber, as shown in Figure 9.

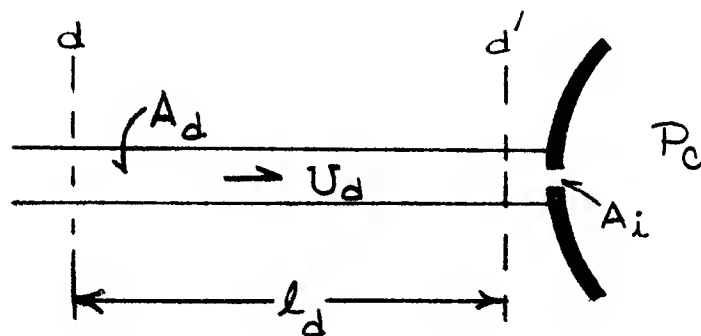


Figure 9 - Discharge Line and Injector

Applying Newton's second law to the discharge line from d to d' , assuming the pressure loss due to friction to be $C_d \frac{\gamma}{2g} U_d^2$,

$$\frac{\gamma l_d}{g} \dot{U}_d = P_d - P_{d'} - C_d \frac{\gamma}{2g} U_d^2$$

We subtract from the above equation the steady state equation

$$0 = \bar{P}_d - \bar{P}_{d'} - C_d \frac{\gamma}{2g} \bar{U}_d^2$$

and introducing the relationship

$$\gamma A U = \dot{W}$$

or

$$\gamma A \dot{U} = \gamma A \dot{u} = \dot{\dot{W}} = \ddot{W}$$

we obtain the result

$$\frac{l_d}{g A_d} \ddot{W} = P_d - P_{d'} - \frac{C_d \bar{W}}{\gamma g A_d^2} \dot{W} \quad (13)$$

Proceeding to the injector we write Bernoulli's equation between d' and the combustion chamber where the pressure is P_c

$$P_{d'} + \frac{\gamma}{2g} U_{d'}^2 = P_c + \frac{\gamma}{2g} U_i^2$$

Again subtracting the steady state equation and replacing \bar{U} in terms of \bar{W} we arrive at the equation

$$p_d' = p_c + \frac{\bar{W}_d}{\gamma g A_d^2} \left(\frac{A_d^2}{A_i^2} - 1 \right) \dot{w}_d \quad (14)$$

Eliminating p_d' between Eqs. (13) and (14) and taking the Laplace transform, the transfer function for the discharge line and injector becomes

$$\dot{w}_d = \frac{p_d(s) - p_c(s)}{\left[\frac{l_d}{g A_d} s + C_d \frac{\bar{W}_d}{\gamma g A_d^2} + \frac{\bar{W}_d}{\gamma g A_d^2} \left(\frac{A_d^2}{A_i^2} - 1 \right) \right]} \quad (15)$$

Its block diagram can then be drawn as in Figure 10.

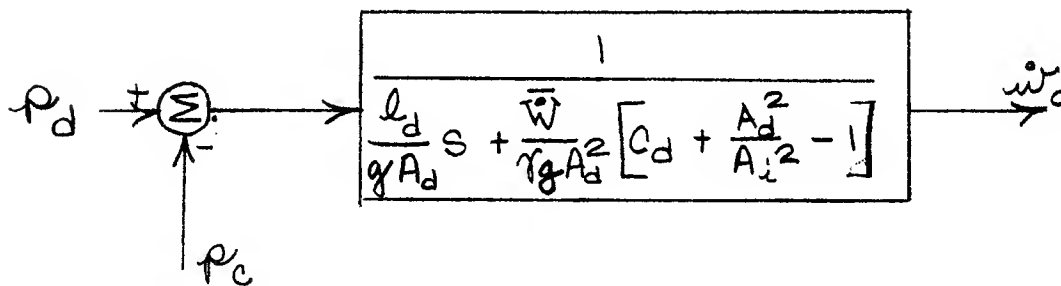


Figure 10-- Block Diagram of Discharge Line and Injector

The ignited gas in the chamber travels through the converging-diverging nozzle which is designed so that sonic speed is reached at its throat. The expansion then takes place supersonically to the exit with the developed thrust F . This process from chamber pressure P_c to thrust F is again dependent on many factors and hence it is usual practice to simplify the result in terms of a thrust coefficient C_F which is a function of the specific heat ratio, the ratio of exit to throat area A_c/A_t and the ratio of exit to chamber pressure P_e/P_c . The equation is then written as

$$F = C_F A_t P_c$$

and its transfer function is

$$\frac{f(s)}{P_c(s)} = C_F A_t \quad (18)$$

The block diagram for the engine can then be draw as in Figure 11.

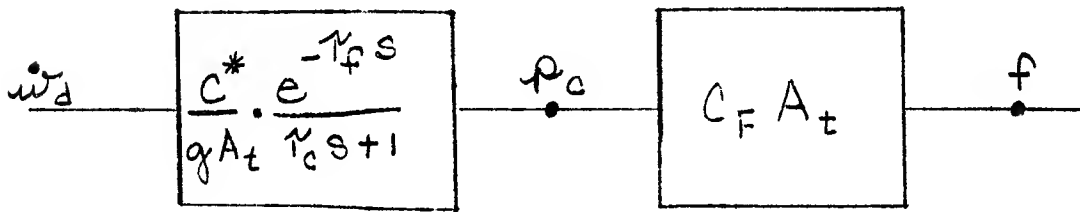


Figure 11 - Block Diagram of Rocket Engine

(e) Structural Dynamics

The dynamical equations for the structure can be established from Figure 2. Since we are interested only in the fluctuation due to the variation in thrust, these equations become

$$M_1 \ddot{y}_1 = f - k(y_1 - y_2) - c(\dot{y}_1 - \dot{y}_2)$$

$$M_2 \ddot{y}_2 = k(y_1 - y_2) + c(\dot{y}_1 + \dot{y}_2)$$

Taking the Laplace transform with zero initial conditions

$$(s^2 M_1 + cs + k) y_1(s) - (cs + k) y_2(s) = f(s)$$

$$-(cs + k) y_1(s) + (s^2 M_2 + cs + k) y_2(s) = 0$$

Thus the transfer functions for the structure become

$$\frac{y_1(s)}{f(s)} = \frac{N_1(s)}{D(s)}, \quad \frac{y_2(s)}{f(s)} = \frac{N_2(s)}{D(s)} \quad (19)$$

where

$$N_1(s) = \begin{vmatrix} 1 & -(cs + k) \\ 0 & (s^2 M_2 + cs + k) \end{vmatrix}$$

$$N_2(s) = \begin{vmatrix} (s^2 M_1 + cs + k) & 1 \\ -(cs + k) & 0 \end{vmatrix}$$

$$D(s) = \begin{vmatrix} (s^2 M_1 + cs + k) & -(cs + k) \\ -(cs + k) & (s^2 M_2 + cs + k) \end{vmatrix}$$

Its block diagram can then appear as in Figure 12.

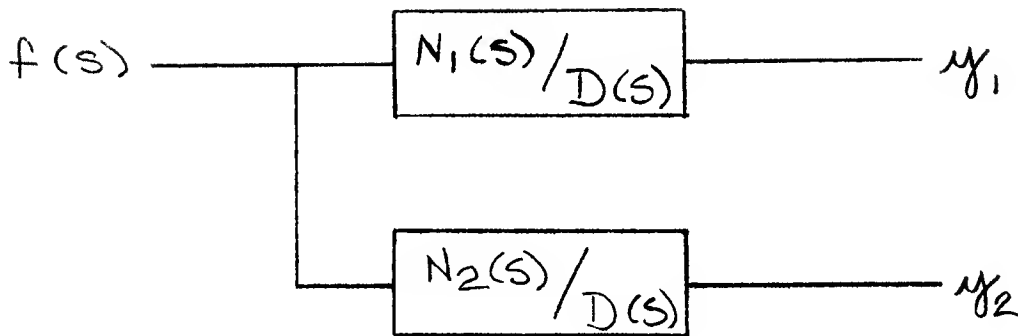


Figure 12 - Block Diagram of Structure

In a more sophisticated approach, the above simplified technique can be replaced by the mode-summation method utilizing generalized coordinates. The deflection at any point is then represented as

$$w(\xi) = \sum_i \phi_i(\xi) q_i(t)$$

where

$$\ddot{q}_i + 2\zeta\omega_i\dot{q}_i + \omega_i^2 q_i = F_i(t)$$

and

$$\phi_i(\xi) = \text{normal mode of the structure}$$

Structural dynamics would still be represented by a block diagram where the thrust \bar{F} is the input and the displacements at 1 and 2 are the output.

System Block Diagram

It is a simple matter now to assemble the various block diagrams into a closed loop circuit shown in Figure 13. System behavior can then be computed by programming on the analog or digital computer.

Computation and Evaluation

Numerical values for the system parameters must be established for the duration of flight of interest to this study. Changes in these parameter values may be incorporated in the computation to establish their effect on the behavior of the system.

"Fix-devices" which have been used successfully are the piston-spring accumulator and the standpipe accumulator at the suction end of the fuel feed line shown in Figure 1. Such devices may be incorporated into the system diagram to study their effect on performance. The increase in the gas pressure P_T in the tank will also help to stabilize the system, in that it will increase the pressure at the pump inlet and reduce cavitation.

Approximate Numerical Values

$$L_f = \frac{l_f}{g A_f} = \frac{40}{32.2 \times 0.40} \approx 3.1$$

$$L_d = \frac{l_d}{g A_d} \approx 0.3$$

$$\frac{\tau l_f}{g L_f} = \frac{90 \times 40}{32.2 \times 3.1} \approx 37.$$

$$\frac{\tau h}{g L_f} \approx 3.7$$

$$\frac{\bar{w}}{\tau g A_f^2} = \frac{1000}{90 \times 32.2 \times 0.40^2} \approx 2.2$$

$$\alpha = \frac{C_f + 1}{L_f} \left(\frac{\bar{w}_1}{\tau g A_f^2} \right) = \frac{1}{3.1} (2.2) \approx 0.72$$

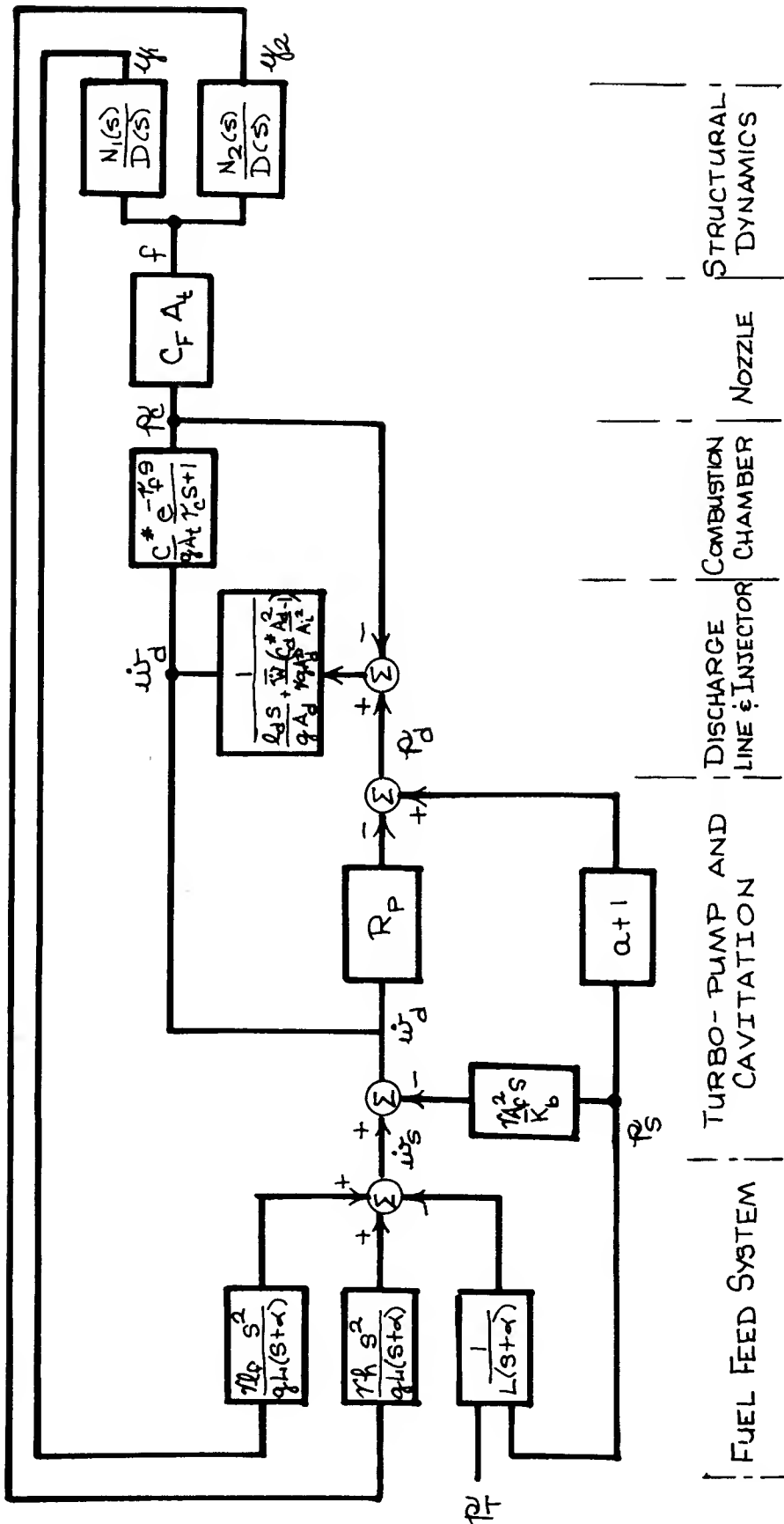


FIG. 13 BLOCK DIAGRAM FOR SYSTEM

$$a+1 \approx 2$$

$$R_p = 90$$

$$R_f = C_f \frac{\bar{W}}{\gamma_g A_f^2} \approx 0$$

$$R_d = C_d \frac{\bar{W}}{\gamma_g A_d^2} \approx 0$$

$$\frac{\bar{W}_d}{\gamma_g A_d^2} \left(\frac{A_d^2}{A_i^2} - 1 \right) \approx 230$$

$$C^*/\gamma A_T \approx 134$$

$$\gamma_c \approx 0.0015$$

$$\gamma_f \approx 0$$

$$C_F A_t \approx 4.3$$

$$\omega^2 = \frac{K_b}{\frac{\gamma}{g} (l_f + h)} \approx 76^2 \text{ for unfavorable condition of 12 cps.}$$

$$\therefore K_b = 76^2 \times \frac{90}{32.2} \times 44 \approx 710,000 \text{ lb/ft}^2$$

$$\frac{\gamma A_f^2}{K_b} = \frac{90 \times .40^2}{710,000} \approx 0.0000204$$

Problems for Students

- (1) With the bulk modulus of the fluid defined as $B = \frac{-dP}{dV/V}$, show that the compliance of the fluid in the pipe of area A is $\frac{\gamma A}{B}$. What is the compliance per unit area for water?
- (2) Derive the transfer function for the standpipe accumulator and indicate how it is fitted into the block diagram of Figure 13.
- (3) Using the mode summation technique, determine the transfer functions for the structural dynamics and draw its block diagram to replace the one in Figure 13.

Observed Natural Frequencies of Titan-2 in Flight

		Time-Sec				
Nat. Freq.		105	115	125	135	145
ω_1	rad/sec	65	68	74	83	105
ω_2	rad/sec	119	136	159	173	174
W_1	= 60,000# = constant					
W_2	= 90,000# @ t = 105 sec.					

$$= \sqrt{\frac{g}{M_1} \left(1 + \frac{M_1}{M_2}\right)}$$

References

1. J. H. Walker, R. A. Winje, K. J. McKenna, "An Investigation of Low Frequency Longitudinal Vibration of the Titan II Missile During Stage 1 Flight," TRW 6438-6001-RV-000, Mar. 26, 1964.
2. Robert S. Wick, "The Effect of Vehicle Structure on Combustion Stability in Liquid-Propellant Rockets," JPL, Progress Report Number 20-248, Dec. 1, 1954.
3. R. G. Dorsch, D. J. Wood, C. Lightner, "Distributed Parameter Analysis of Pressure and Flow Disturbances in Rocket Propellant Feed Systems," NASA TN D-3529, Aug. 1966.
4. R. G. Rose, J. A. Staley, A. K. Simson, "A Study of System-Coupled Longitudinal Instabilities in Liquid Rockets," Air Force Rocket Propulsion Lab AFRPL-TR-65-163, Sept. 1965.

Notes for Instructor

The mode summation method assumes the displacement at any point to be expressible as

$$y(x, t) = \sum_i q_i(t) \phi_i(x)$$

where $\phi_i(x)$ is the i^{th} normal mode shape and $q_i(t)$ is the generalized coordinate for the i^{th} mode satisfying the equation

$$\ddot{q}_i(t) + 2\zeta_i \omega_i \dot{q}_i(t) + \omega_i^2 q_i(t) = \frac{1}{M_i} \int_0^l F(x, t) \phi_i(x) dx$$

In the above equation ω_i is the natural frequency, ζ_i the damping factor, $M_i = \int_0^l M(x) \phi_i^2(x) dx$ the generalized mass, all for the i^{th} mode, and $F(x, t)$ is the applied force.

For the Pogo problem $F(x, t)$ is applied at the end of the missile $x = 0$, and the generalized force becomes

$$\int_0^l F(x, t) \phi_i(x) dx = F(t) \phi_i(0)$$

The Laplace transform of the displacement is

$$y(x, s) = \sum_i q_i(s) \phi_i(x)$$

where

$$q_i(s) = \frac{f(s) \phi_i(0)}{M_i [s^2 + 2\zeta_i \omega_i s + \omega_i^2]}$$

Thus at $x = x_1$ and x_2 we have

$$y_1(s) = \sum_i \frac{f(s) \phi_i(0) \phi_i(x_1)}{M_i (s^2 + 2\zeta_i \omega_i s + \omega_i^2)}$$

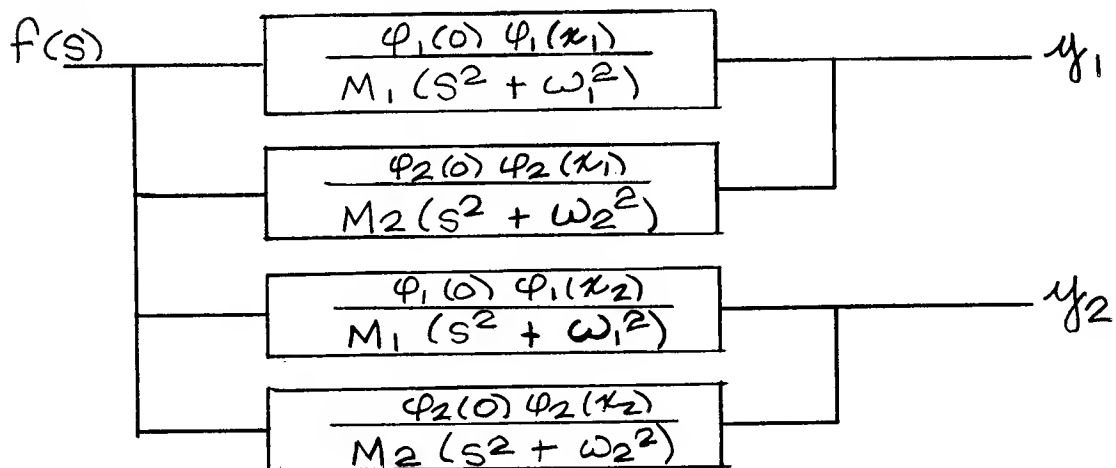
$$y_2(s) = \sum_i \frac{f(s) \phi_i(0) \phi_i(x_2)}{M_i (s^2 + 2\zeta_i \omega_i s + \omega_i^2)}$$

Since data are given for only the first two modes the result with zero damping becomes

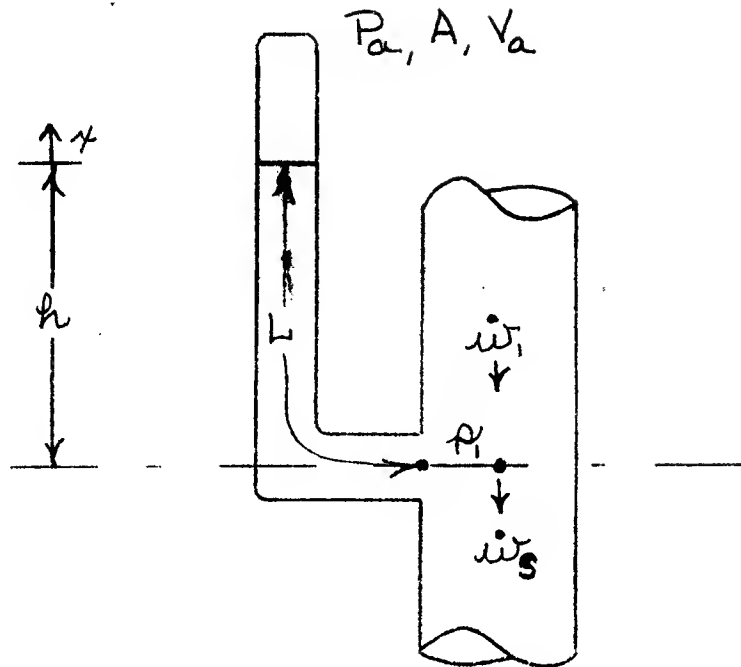
$$y_1(s) = f(s) \left\{ \frac{\varphi_1(0) \varphi_1(x_1)}{M_1(s^2 + \omega_1^2)} + \frac{\varphi_2(0) \varphi_2(x_1)}{M_2(s^2 + \omega_2^2)} \right\}$$

$$y_2(s) = f(s) \left\{ \frac{\varphi_1(0) \varphi_1(x_2)}{M_1(s^2 + \omega_1^2)} + \frac{\varphi_2(0) \varphi_2(x_2)}{M_2(s^2 + \omega_2^2)} \right\}$$

The block diagram then becomes



which replaces Figure 12.

Equations for the Standpipe

Newton's second law applied to the fluid in the standpipe is

$$\gamma L A \ddot{x} = (\bar{P}_i + p_i)A - (\bar{P}_a + p_a)A - \gamma A(h+x)$$

Eliminating the steady-state equation we are left with

$$\gamma L \ddot{x} = p_i - p_a - \gamma x \quad (1)$$

The trapped air in the standpipe must obey the gas law

$$(\bar{P}_a + p_a)(\bar{V} - Ax)^n = \bar{P}_a \bar{V}^n$$

Expanding by the binomial theorem and neglecting second order terms, we have

$$\therefore p_a = \frac{n \bar{P}_a}{\bar{V}} Ax$$

(2)

Eq. (1) now becomes

$$\gamma L \ddot{x} + \left(\frac{\gamma \bar{P}_a A}{\bar{V}} + \gamma \right) x = p_1 \quad (3)$$

We next introduce continuity of flow

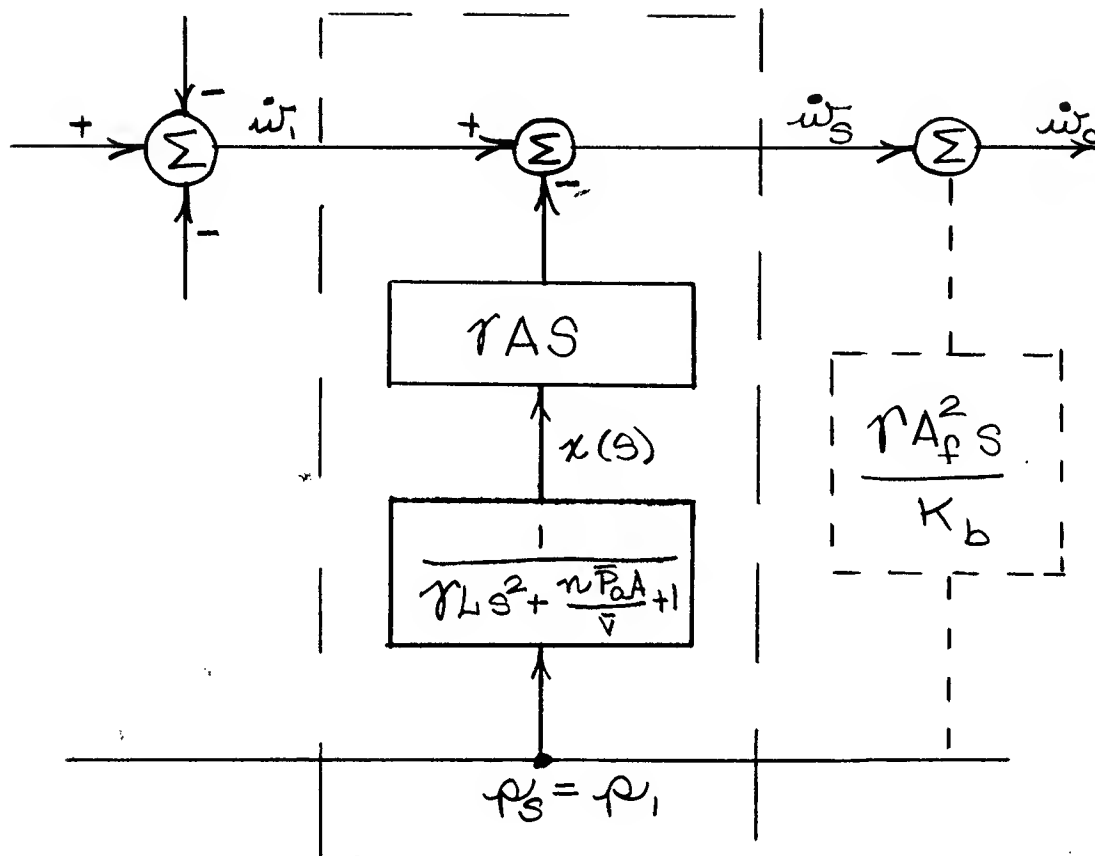
$$\dot{w}_s = \dot{w}_1 - \gamma A \dot{x} \quad (4)$$

The transfer functions from Eq. (3) and (4) are

$$x(s) = \frac{1}{\gamma L s^2 + \left(\frac{\gamma \bar{P}_a A}{\bar{V}} + \gamma \right)} p_1(s) \quad (3')$$

$$\dot{w}_s(s) = \dot{w}_1(s) - \gamma A s x(s) \quad (4')$$

It should now be recognized that we can let $p_1 = p_s$ and that \dot{w}_θ in Figure 3 must be changed to \dot{w}_1 . Thus the block diagram for the standpipe becomes



and its position in the large block diagram is also indicated.